γ vibrational band and quasiparticle excitations in ^{80}Sr

T. A. Sienko,[1,2] C. J. Lister,[2] and R. A. Kaye[1]
[1]*Department of Chemistry and Physics, Purdue University Calumet, Hammond, Indiana 46323, USA*
[2]*Physics Division, Argonne National Laboratory, 3700 South Cass Avenue, Argonne, Illinois 60439, USA*
(Received 24 January 2003; published 25 June 2003)

Non-yrast states in ^{80}Sr were populated in the ^{24}Mg(^{58}Ni,2p)^{80}Sr reaction at 200 MeV and their γ decays investigated using Gammasphere, in order to investigate shape softness and quasiparticle excitations. A large data set was collected which was A and Z gated, using the Argonne Fragment Mass Analyzer and a focal plane ion chamber. The excellent channel selection enhanced the sensitivity to energetically nonfavored configurations. Several new rotational bands were found, and many conflicts between previous experiments were resolved. In particular, the gamma vibrational band is now clearly delineated, and more than ten quasiparticle bandheads have been identified. At the highest spins, evidence for a long-predicted shape change was found.

DOI: 10.1103/PhysRevC.67.064311 PACS number(s): 23.20.En, 23.20.Lv, 21.10.Hw, 27.50.+e

I. INTRODUCTION

The deformed nuclei of the neutron deficient $A\sim80$ region are interesting for investigating the microscopic underpinning of collective rotational behavior in general, as they lie in the middle of the *f-p-g* shell model space which is large enough to support substantial collectivity, with quadrupole transitions of 100's of Weisskopf units in the ground-state bands, but which is small enough that individual particles in specific orbits can strongly modulate that collectivity. The potential-energy surfaces of nuclei in the region are soft, both to elongation β and triaxiality γ, so shape polarization is easy and shape vibrational excitations are expected to be low lying. Measuring and calculating these shapes and their vibrations provide a challenging contemporary test of our understanding of nuclear structure.

^{80}Sr is a classic soft deformed rotor in the $A\sim80$ region. It was one of the first nuclei to be identified as having a large quadrupole deformation in a pioneering heavy-ion study by Morinaga's Munich group [1] and has since been extensively studied experimentally, both ''in beam'' [2–7] and through the decay of ^{80}Y [8–10]. Many of the techniques now commonly used for studying neutron-deficient nuclei far from stability were developed for investigating this nucleus and its neighbors [1,2,5]. Numerous theoretical investigations have also been made [11–17] using a variety of approaches, including the interacting boson model, relativistic mean-field calculations, Hartree-Fock-Bogoliubov calculations, and diverse microscopic-macroscopic Strutinski-type models. The seminal Woods-Saxon calculations of Nazarewicz *et al.* [13] were very important in revealing the importance of deformed shell gaps in establishing the physics of nuclei throughout this region, including their ground-state shapes, band terminations, and their backbending characteristics. One prediction, that of superdeformation, has recently been verified [18]. Another long-standing prediction, that of an abrupt change from near-prolate to near-oblate shapes at high spin, appears to be verified in this work.

Despite the extensive experimental work on ^{80}Sr, puzzles remain concerning vibrational modes and the spins and parities of the lowest quasiparticle excitations. There are inconsistencies between some of the published ''in-beam'' studies and with the decay work. The present experiment was aimed at favorably populating low-spin, non-yrast states in order to resolve some of these discrepancies and clarify the lowest modes of excitation, particularly the collective vibrational states.

II. EXPERIMENTAL METHOD

States in ^{80}Sr were populated using the ^{24}Mg(^{58}Ni,2p)^{80}Sr reaction. The ^{58}Ni beam at 200 MeV was accelerated by the ATLAS superconducting linear accelerator at Argonne National Laboratory [19]. Inverse kinematics were used to enhance the collection of residues near zero degrees, and to improve Z separation in the focal plane ion chamber. A 0.8-mg/cm^2 foil of $>$99.5% isotopically enriched ^{24}Mg was used, with a 5-μg/cm^2 ^{12}C charge reset foil positioned 10 cm downstream. Gamma rays were detected in Gammasphere [20], which contained 100 large ($>$70% relative efficiency) hyperpure germanium detectors, each mounted in a BGO Compton-suppression shield. The absolute singles efficiency was $\sim$9% for 1.33-MeV gamma rays, and the peak-to-total ratio $>$55%. Reaction products which recoiled inside a rectangular aperture of $0.8\times1.4°$ around zero, passed into the Argonne Fragment Mass Analyzer (FMA) [21], where the noninteracting beam was rejected at the 10^{-7} level, and the residues dispersed across a 10-cm focal plane according to A/q, their mass/atomic charge state ratio. For this experiment, the FMA efficiency was estimated to be $\sim$5%. Ions crossing the focal plane were detected in a two-dimensional position sensitive foil-and-channel-plate system of 8×10 cm with the foil made of aluminized formvar [22]. Mechanical slits positioned upstream of the focal plane were used to select residues with $A/q=80/25=3.20\pm0.01$, thus reducing the downstream count rate to $<10^4$ cps. The ions were stopped in a three electrode, 30-cm-deep, ion chamber operated at 25 torr of isobutane. The time correlations between the accelerator rf clock and all detectors were recorded to allow time-random events to be categorized. The experiment had a triggering method in which an ''event'' was hardware selected and consisted of a Compton-suppressed germanium event (taken at the VXI crate level) in coincidence with an ion traversing the focal

 ©2003 The American Physical Society

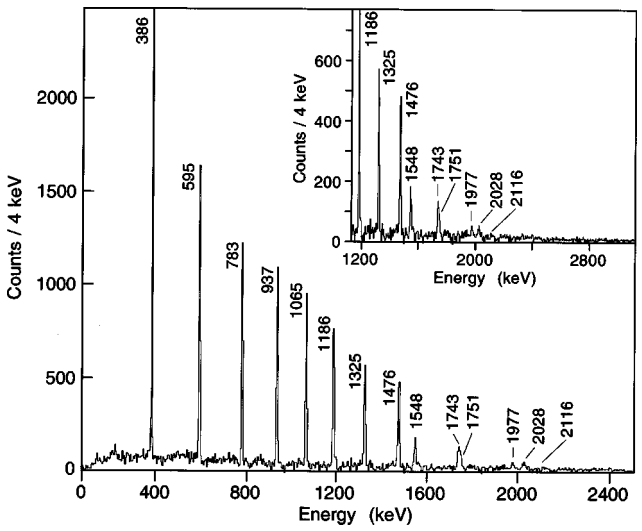

FIG. 1. A sample of the high quality γ-γ data from this experiment, showing a single gate set on the 1579-keV $J=18\rightarrow16$ decay in the yrast line. Above this point ''forking'' of the band occurs; the yrast sequence has a backbend which has been predicted to correspond to a change from near-prolate to near-oblate shape.

plane between 700 and 1000 ns later. Only when this condition was satisfied were events digitized and read out. This triggering method considerably reduced deadtime and allowed Gammasphere to be operated in a residue-gated, low-multiplicity mode; for this experiment multiplicity 2 was selected. In post-run analysis, it was noticed that due to differences in length of the Gammasphere's signal cables, some detectors did not satisfy the hardware trigger requirements, and about 30% of good events were lost.

Data were collected for 48 ''live-time'' hours, with an

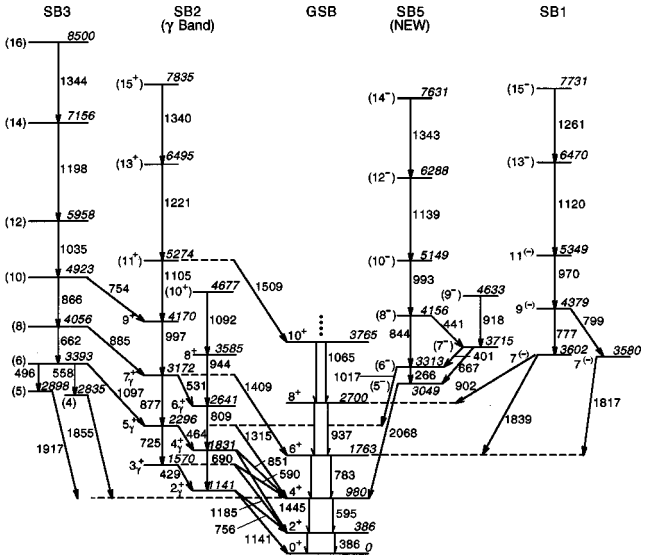

FIG. 2. The decay scheme of low-lying states in ^{80}Sr. Many particle-hole excited configurations are evident near 3 MeV of excitation. Only the collective gamma-vibrational band lies low in excitation, with a bandhead at 1.141 MeV. The continuation of the bands to high spin is given in Table I and is not shown in the figures.

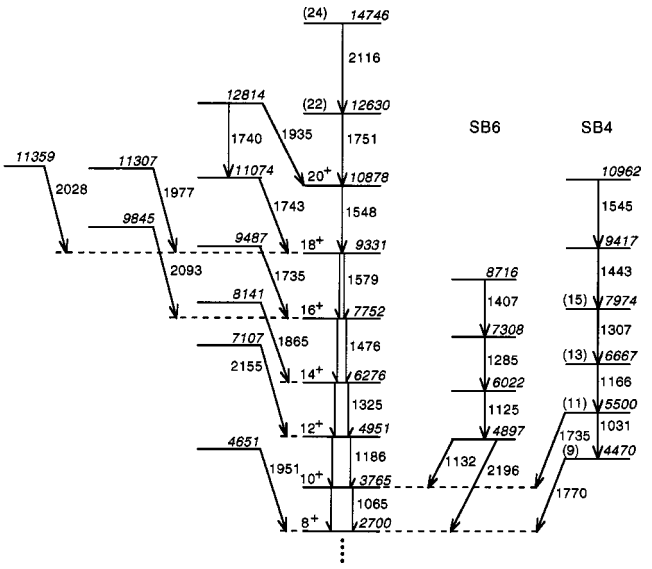

FIG. 3. The decay scheme of highly excited states associated with the ground-state band. Above spin $J=18$, many particle-hole excitations approach the yrast line and the decay pattern becomes very complicated. For clarity, several other bands shown in Fig. 2 continue to high spin and are not shown in this figure.

average beam current of 5 pnA. The ion chamber data were corrected for small time-dependent gain drifts (at ~2% level) and then sorted into an energy-loss vs energy matrix. The Bragg curves for scattered beam particles, ($Z=28$) and ^{77}Rb ($Z=37$), (arriving at the focal plane as an A/q ambiguity with $A/q=77/24$), ^{80}Sr ($Z=38$), ^{80}Y ($Z=39$), and ^{80}Zr ($Z=40$), could be traced. The ^{80}Sr ions were most intense by more than an order of magnitude. The energy-loss loci were parametrized and ''linearized'' to create an energy-independent energy-loss signal which could be used to separate mass $A=80$ isobars. An optimum ''strontium'' gate was selected, as were gates for yttrium and rubidium. The zirco-

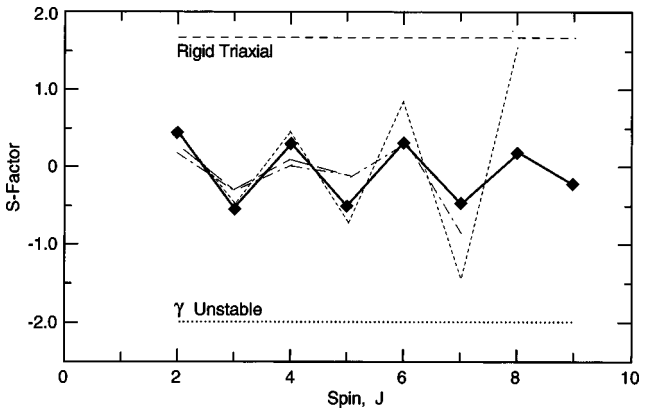

FIG. 4. A plot of the $S(J,J\text{-}1,J\text{-}2)$ factor of Zamfir and Casten (Ref. [27]) as a function of spin for even-even nuclei ^{80}Sr (solid), ^{82}Sr (short-dash) (Ref. [24]), ^{78}Kr (dash-dot) (Ref. [25]), and ^{84}Zr (long-dash) (Ref. [23]). All show similar characteristics, with an odd-even splitting and average values near zero, characteristic of triaxial, but soft, shapes. The S factor for ^{80}Sr seems particularly constant with spin.

nium locus was of very low intensity and was well separated from that of strontium. Gamma rays, in time coincidence with each of the ions, were identified and sorted into time-random-subtracted prompt energy-angle and energy-energy matrices that were Doppler corrected. Due to the symmetry of Gammasphere, the effective recoil velocity could be empirically determined to match up-shifted and down-shifted photopeaks, depending on detector angle. The effective velocity was $v/c=0.051$. Further refinement to improve the Doppler correction included event-by-event relative velocity correction, using the ion chamber energies, and for the 60 detectors around the girth of Gammasphere near 90°, the segmentation of the germanium crystals was used to identify ''upstream,'' ''middle,'' and ''downstream'' gamma-ray hits (the ''upstream'' and ''downstream'' hits being effectively $\pm 2.8°$ different from the mechanical detector angle). Even so, after this sophisticated correction, the photopeaks had ~6-keV full width at half maximum at 1 MeV, three times the intrinsic resolution, reflecting the importance of more position-sensitive detectors in the future.

The matrices of data were then ''purified'' by subtracting scaled-down matrices of neighboring isobars, with a normalization chosen to exactly remove the strongest clean ''breakthrough'' transitions. In this particular case, ^{80}Sr was so intense that these subtractions were $\lesssim 5\%$. At the end of this analysis, matrices could be produced in which almost all of the transitions appeared to be associated with ^{80}Sr, allowing a catalog of ^{80}Sr gamma rays to be created. The 386-keV, $J^\pi=2^+\rightarrow 0^+$, transition photopeak had more than 10^6 counts. About 60% of the events had more than one gamma ray in prompt coincidence. For most of these transitions, the angular distribution could be studied and coincident gamma rays identified. Figure 1 shows a single window from the coincidence matrix, on the high-lying 1579-keV $J^\pi=18^+\rightarrow 16^+$ transition, where the quality of the data can be seen. The decay scheme developed in this work is shown in two parts as it is complicated. The low-spin regime and bandheads are in Fig. 2, and the fragmentation of the high-spin sequences are shown in Fig. 3.

The number of detectors at each angle is not the same in Gammasphere, and the response of each detector slightly different, so similarly-sorted ^{152}Eu and ^{56}Co source spectra were used to create a set of angle normalization factors and efficiency curves. The measured isotropy of the 386-keV ground-state decay, caused by vacuum deorientation, and always seen in this type of study, further verified the normalization. The validity of the angle normalization was checked by measuring the well-known cascade of $E2$ decays in the ground-state band. These transitions also provided a measure of the spin-dependent alignment. The source data were also used for relative gain matching, though the absolute spectrum after Doppler correction was slightly shifted (0.2 keV) to match the well-measured low-lying ^{80}Sr transitions from the ^{80}Y radioactive decay experiments. This correction probably arises from a small mechanical misalignment of the target relative to the exact center of Gammasphere. Table I is a compilation of all the known transitions. As there are many gamma rays, they are grouped by bands, where the assignments are known. The weakest transitions have only energies, intermediate transitions and those forming complex multiplets in the spectrum show the a_2 angular distribution coefficient, and the stronger transitions have both a_2 and a_4 coefficients.

III. RESULTS AND DISCUSSION

A. Gamma vibrational band

It is surprising that there is considerable uncertainty concerning spin and structural assignments for some of the very lowest-lying nonyrast states. Our clean, channel-selected data are particularly useful in this respect. The lowest nonyrast excitation we find is the gamma vibrational band, consistent with the gamma soft potential-energy surfaces always calculated for ^{80}Sr (e.g., Refs. [12,13]). The $J^\pi=K^\pi=2^+$ bandhead has been known for some time [8] at 1141 keV, as it is populated in beta decay. A recent, more detailed study of the ^{80}Y beta decay following mass separation by Döring *et al.* [10] supported this assignment, and found candidates for higher-lying multiphonon vibrational states. Decaying to the $J=2_2$ bandhead, Davie *et al.* [4] reported an odd-spin sequence, starting at $J=3$ at 1570 keV, based on an angular distribution fit to the 1185-keV decay to the ground-state band which favored a $\Delta J=1$ decay with a large positive mixing ratio. The Döring *et al.* [10] investigation found consistency with this assignment and reported candidates for the first odd-spin member of the gamma band, and one candidate for the even-spin sequence of this band. In contrast, Winchell *et al.* [7] concluded the 1570-keV state had $J=4$, without discussing the data supporting the change of assignment. In the present ''in-beam'' data set we have observed the even spin members of the band to spin $J=10$ which interleave and link with Davie's odd spin cascade, as is shown on the left side of Fig. 2. These new states, and their linking transitions, confirm the original spin assignments [3,4,10], and show the Winchell *et al.* assignment to be incorrect. We were able to extend the odd-spin cascade beyond the 1339-keV transition reported by Winchell *et al.* by three more states to $J^\pi=(21^+)$, with a series of quadrupole decays of energies 1507, 1615, and 1752 keV given in Table I.

The proposed scheme is now very similar to the gamma bands recently explored in detail in neighboring ^{84}Zr [23], ^{82}Sr [24], and ^{78,80}Kr [25,26]. Analysis of all these bands using the $S(J,J-1,J-2)$ factors of Zamfir and Casten [27] show an odd-even staggering around zero value, as shown in Fig. 4. Although there is an odd-even spin effect, the ''S'' factor remains quite constant in ^{80}Sr, compared to the neighbors and small in magnitude. The behavior is intermediate between a rigid triaxial ''S'' factor, of $+1.67$ and that of complete gamma softness, where $S=-2.0$ is expected. The positions of the gamma band members relative to the ground-state band, provide information on the mean triaxiality. In a rigid model, they would indicate the triaxiality was ~20° for ^{80}Sr. However, the small value of the ''S'' factor indicates that the amplitude of vibrations about the mean value is large.

The clear development of a clear gamma rotational band ''in-beam'' now balances the evidence from β-decay work [10], where population of high-lying nonyrast states is ob-

TABLE I. A compilation of the gamma rays and their properties associated with ^{80}Sr which were studied in this work. The intensities are normalized to have 1000 units decaying to the ground state. The gamma rays are grouped according to the band in which they have been assigned. A few transitions are known to be in ^{80}Sr, but could not be reliably placed.

E_{state} (keV)	J_i^π	J_f^π	E_γ (keV)	I_γ[a]	a_2	a_4
GSB						
385.6 (2)	2^+	0^+	385.6 (2)	929 (23)	.01 (1)	−.03 (1)
980.2 (3)	4^+	2^+	594.6 (2)	799 (20)	.12 (1)	−.04 (1)
1 763.0 (3)	6^+	4^+	782.8 (2)	636 (16)	.22 (1)	−.06 (1)
2 699.7 (4)	8^+	6^+	936.8 (2)	486 (12)	.26 (1)	−.11 (1)
3 765.1 (4)	10^+	8^+	1065.4 (2)	369 (10)	.27 (1)	−.11 (2)
4 951.5 (5)	12^+	10^+	1186.3 (2)	279 (11)	.24 (1)	−.08 (2)
6 276.1 (5)	14^+	12^+	1324.6 (2)	168 (5)	.32 (2)	−.02 (3)
7 751.9 (6)	16^+	14^+	1475.9 (2)	99 (3)	.33 (3)	−.09 (4)
9 330.7 (6)	18^+	16^+	1578.7 (3)	59 (3)	.31 (5)	−.13 (7)
10 878.5 (7)	20^+	18^+	1547.8 (3)	39 (2)	.30 (6)	−.20 (9)
12 630 (1)	(22^+)	20^+	1751.2 (7)	10 (1)		
14 746 (1)	(24^+)	(22^+)	2116.5 (7)	4 (1)		
SB1						
3 601.9 (3)	$7^{(-)}$	8^+	902.1 (3)	9 (1)	−.14 (17)	−.12 (22)
	$7^{(-)}$	6^+	1839.0 (2)	50 (2)	−.40 (5)	−.04 (6)
3 580.3 (3)	$7^{(-)}$	(5)	683.1 (3)	12 (1)	.07 (9)	
	$7^{(-)}$	6^+	1817.0 (3)	71 (2)	−.10 (4)	−.07 (5)
4 379.0 (3)	$9^{(-)}$	$7^{(-)}$	776.7 (2)	57 (2)	.12 (5)	.00 (7)
	$9^{(-)}$	$7^{(-)}$	799.1 (2)	50 (1)	.24 (4)	−.04 (5)
5 349.2 (3)	$11^{(-)}$	$9^{(-)}$	970.3 (2)	87 (2)	.23 (2)	−.09 (3)
6 470.6 (4)	$13^{(-)}$	$11^{(-)}$	1120.0 (2)	79 (3)	.25 (3)	−.12 (3)
7 731.4 (5)	$15^{(-)}$	$13^{(-)}$	1260.8 (2)	67 (2)	.29 (5)	−.02 (6)
9 099.7 (5)	$17^{(-)}$	$15^{(-)}$	1368.3 (2)	59 (2)	.34 (4)	−.23 (6)
10 539.6 (6)	$19^{(-)}$	$17^{(-)}$	1439.9 (4)	40 (2)	.19 (4)	.07 (5)
12 072.8 (8)	$21^{(-)}$	$19^{(-)}$	1533.2 (5)	16 (3)	.38 (7)	−.05 (9)
13 723.3 (9)	(23^-)	(21^-)	1650.6 (4)	9 (1)		
15 577 (1)	(25^-)	(23^-)	1853.2 (5)	5 (1)		
SB2 (gamma band)						
1 141.0 (2)	2^+	2^+	755.9 (3)	25 (1)	.07 (4)	−.02 (5)
		0^+	1140.8 (2)	71 (2)	.01 (12)	.01 (15)
1 570.3 (2)	3^+	2^+	429.1 (2)	19 (1)	−.03 (9)	−.02 (10)
		4^+	590.2 (3)	9 (1)		
		2^+	1185.0 (2)	49 (12)		
1 831.4 (2)	4^+	2^+	690.4 (2)	16 (1)	.15 (7)	−.08 (9)
		4^+	851.5 (2)	15 (1)	−.06 (9)	13 (11)
		2^+	1444.6 (4)			
2 295.6 (2)	5^+	4^+	463.9 (2)	10 (1)		
		3^+	725.2 (2)	70 (2)	.19 (3)	−.08 (4)
		4^+	1316.0 (2)	80 (2)	.20 (4)	.04 (5)
2 640.7 (3)	6^+	4^+	809.3 (2)	19 (1)	.07 (9)	−.34 (12)
3 172.2 (3)	7^+	6^+	530.8 (2)	15 (4)		
		5^+	876.6 (2)	80 (2)	.20 (3)	−.05 (4)
		6^+	1408.8 (5)			
3 584.5 (4)	8^+	6^+	943.8 (2)	31 (1)	.23 (6)	.04 (8)
4 169.5 (4)	9^+	7^+	997.4 (2)	72 (3)	.23 (5)	−.14 (7)
4 676.8 (8)	10^+	8^+	1092.3 (7)	19 (3)	.25 (12)	
5 274.4 (4)	11^+	9^+	1104.9 (2)	48 (2)	.22 (4)	−.14 (6)
		10^+	1508.7 (3)	21 (3)		
6 495.4 (5)	13^+	11^+	1221.0 (3)	51 (2)	.19 (5)	−.05 (6)
7 831.5 (6)	(15^+)	13^+	1340.0 (3)	18 (1)	.34 (12)	

TABLE I. (*Continued*).

E_{state} (keV)	J_i^π	J_f^π	E_γ (keV)	I_γ[a]	a_2	a_4
7 867.1 (6)	(15^+)	(13^+)	1371.7 (3)	13 (2)		
9 340.2 (5)	(17^+)	(15^+)	1474.1 (4)	14 (2)		
	(17^+)	(15^+)	1507.4 (5)	9 (2)		
10 955.5 (7)	(19^+)	(17^+)	1615.3 (4)	14 (1)		
12 708 (1)	(21^+)	(19^+)	1752 (1)	3 (1)		
SB3						
2 835.0 (8)	(4)	4^+	1854.8 (7)	25 (2)	.20 (8)	−.21 (11)
2 897.6 (4)	(5)	4^+	1917.4 (3)	22 (1)	−.27 (11)	−.11 (15)
3 893.2 (3)	(6)	(5)	496.0 (2)	19 (1)		
		(4)	558.1 (2)	9 (1)		
		5^+	1097.3 (3)	42 (3)	−.31 (7)	−.12 (11)
4 056.1 (2)	(8)	(6)	662.3 (2)	59 (2)	.23 (3)	−.07 (3)
		7^+	884.7 (2)	56 (2)	−.11 (5)	.11 (7)
4 922.8 (3)	(10)	9^+	754.0 (3)	17 (1)		
		(8)	866.3 (2)	72 (2)	.28 (3)	.01 (4)
5 958.1 (4)	(12)	(10)	1035.3 (2)	68 (3)	.32 (5)	.05 (7)
7 156.1 (4)	(14)	(12)	1198.0 (2)	51 (2)	.24 (4)	−.03 (5)
8 499.8 (5)	(16)	(14)	1343.7 (2)	32 (1)	.30 (4)	−.06 (5)
9 882.1 (6)	(18)	(16)	1382.3 (5)	16 (1)	.38 (12)	
SB4						
4 470.2 (5)	(9)	8^+	1770.5 (3)	18 (1)	−.26 (13)	.02 (16)
5 500.5 (5)	(11)	(9)	1030.8 (4)	21 (3)	.30 (8)	−.25 (11)
		10^+	1734.6 (6)	21 (3)	.10 (6)	−.20 (8)
6 666.9 (5)	(13)	(11)	1166.4 (2)	51 (2)	.21 (4)	−.19 (5)
7 974.1 (6)	(15)	(13)	1307.2 (3)	24 (1)	.33 (9)	−.23 (13)
9 417.3 (7)			1443.2 (4)	14 (1)		
10 962.3 (9)			1545.1 (6)	13 (2)		
SB5 (new)						
3 048.5 (5)	(5^-)	4^+	2068.3 (4)	8 (1)	−.48 (17)	−.33 (23)
3 313.3 (3)	(6^-)	(5^-)	266.2 (2)	15 (1)	−.55 (8)	−.04 (11)
		5^+	1017.2 (2)	23 (1)	.07 (8)	.03 (11)
3 714.7 (3)	(7^-)	(6^-)	401.2 (2)	12 (1)	−.52 (13)	.07 (20)
		(5^-)	666.6 (3)	19 (1)	.34 (11)	.05 (16)
4 156.3 (3)	(8^-)	(7^-)	441.0 (3)	7 (1)		
		(6^-)	843.6 (2)	29 (1)	.23 (6)	.03 (8)
4 632.6 (4)	(9^-)	(7^-)	918.0 (2)	19 (1)	.38 (9)	−.26 (12)
5 149.1 (4)	(10^-)	(8^-)	992.8 (3)	40 (3)	.03 (13)	.11 (18)
6 288.3 (5)	(12^-)	(10^-)	1139.2 (2)	28 (3)		
7 631.1 (5)	(14^-)	(12^-)	1342.8 (3)	9 (2)		
SB6						
4 896.7 (4)		10^+	1132.4 (3)	43 (2)	.26 (5)	−.10 (7)
		8^+	2195.7 (5)	14 (1)		
6 022.0 (6)			1125.3 (5)	23 (2)	.34 (5)	.00 (7)
7 307.6 (9)			1285.4 (6)	24 (3)		
8 716 (1)			1407.2 (4)	22 (2)		
Other transitions in decay scheme						
4 650.5 (6)	(9)	8^+	1 950.8 (4)	14 (1)	.26 (18)	−.32 (25)
7 106.8 (6)		12^+	2 155.4 (4)	14 (1)		
8 141 (1)		14^+	1 865 (1)	3 (2)		
9 323.4 (9)		(15^-)	1 592.0 (8)	8 (2)	.40 (25)	
9 486.9 (7)		16^+	1 735.0 (5)	22 (5)		
9 844.8 (7)		16^+	2 092.9 (5)	7 (1)	−.12 (20)	

TABLE I. (*Continued*).

E_{state} (keV)	J_i^π	J_f^π	E_γ (keV)	I_γ[a]	a_2	a_4
11 073.5 (7)		18^+	1 742.9 (4)	12 (1)		
11 307 (1)		18^+	1 976.6 (9)	2 (1)		
11 358.7 (9)		18^+	2 028.0 (7)	6 (1)		
12 813.8 (6)		(20)	1 740.2 (5)	10 (3)		
		(20)	1 935.4 (6)	6 (1)		

[a]Normalized to make the flux to the ground state equal to 1000 units.

served which have decay characteristics consistent with being members of two- and even three-phonon vibrational multiplets.

B. Sideband SB3

Davie *et al.* [4] reported a cascade of $E2$ transitions decaying into the lower members of the gamma band, with a bandhead of unknown spin, J, at 3639 keV. The band was labeled SB3. Winchell *et al.* [7] observed the same cascade of gamma rays, but placed the bandhead at 3394 keV, fixed by three separate decay paths. They allocated a spin/parity of $J^\pi = 7^-$ to this state. In the present study, we find the decay paths proposed by Winchell *et al.* to be correct, but differ over spin assignment. The decay of this structure is to positive parity states, mainly in the gamma band. The interband transitions, for example the clean 884-keV decay, have angular distributions which are rather isotropic, indicating mixed multipolarity decays of $E2/M1$ type, but the data are not of sufficient quality to rigorously assign the parity to the band, although an even spin sequence is strongly favored. Even spin bands with similar decay patterns have been suggested in several neighboring nuclei [28], although negative parity has been proposed. With our spin assignments for the gamma band discussed in Sec. III A, we set the bandhead spin to be most likely $J=(6)$ at 3393 keV. We could follow the cascade as far as the ''upbend'' state at 9882 keV, but could not confirm the higher transitions which were reported by Winchell *et al.* [7]. From an interpretation standpoint, the lack of a parity assignment is unfortunate. An even spin, positive parity sequence provides a natural explanation for the odd-even staggering in the $S(4,3,2)$ plot discussed in the previous section. An interaction between the even members of SB3 and the gamma band, causing repulsion at the ~50-keV level, suppresses the observed staggering in the $S(4,3,2)$ factor. Alternatively, were the band of negative parity, the members would interleave rather well with the members of SB1 with a uniform signature splitting pattern. Under this interpretation it is possible that SB3 could be the missing even spin members of that rotational band.

C. Candidates for negative-parity excitation

The most strongly populated core excitation reported by Davie *et al.* [4] was a cascade which de-excited into the ground-state band at spin $J^\pi = 6^+$. The two high energy ''decay-out'' transitions of 1817 and 1839 keV were reported to be inconsistent with pure dipole radiation, both having very large negative a_2 and large positive a_4 angular distribution coefficients. It was suggested the band had positive parity and a bandhead assignment of $J^\pi = 7^+$, although a ''folded'' $J^\pi = 5^+$ assignment would be equally consistent with the measurement. For many years this result has remained a puzzle, as most neighboring nuclei have been found to have negative parity bands as the most strongly excited non-yrast states. The angular distributions measured by Winchell *et al.* were completely different from Davie's, with much smaller coefficients. The 1839-keV decay appeared to be fully consistent with a pure dipole decay. Our measurements are quite close to Winchell's (Table I of both papers) and in our data both 1817- and 1839-keV decays appear consistent with pure dipole decays. While dipole decay by no means proves the decay is pure $E1$, and thus the band has negative parity, the experimental data which led to the initial positive parity assignment are inconsistent with the new large data sets, opening the question of the parity of this band. In addition, we have confirmed the decay branch to the $J=8$ member of the ground-state band through the 902-keV transition, excluding a ''folded'' spin sequence. High-energy pure dipole decays are frequently found as parity-changing interband transitions, so with no other data available, negative parity would become experimentally favored, setting the bandhead at $J^\pi = 7^{(-)}$. It is very difficult to construct a positive parity high-spin bandhead from the states available near the Fermi surface. However, several high-spin negative bandheads can be easily constructed, with a $g_{9/2}$ particle and one in the *fp* shell, also favoring this assignment. Preliminary results from a measurement of the polarization of these transitions [29] using ''clover'' detectors to measure the asymmetry of Compton scattering further indicate that the 1817- and 1839-keV gamma rays are indeed of $E1$ character.

A completely new set of states has been found decaying into the ground-state band at spin $J=4$, as is shown on the right of Fig. 2. It is surprising that these states have not been seen before, as they are quite strongly populated. Figure 5 shows a coincident window from the new band. The ''decay-out'' transition is a high-energy, 2068-keV, dipole transition, suggesting negative parity. Above it, the lowest energy transition known in ^{80}Sr, at 266 keV is located. This unusual pattern, a ~2000-keV decay with a ~200-keV precursor, is found in both isotones and isotopes of ^{80}Sr, always associated with negative parity [23–25,28]. Thus a negative parity assignment for this band also seems likely.

D. High-spin ground-state band

Although this experiment was not specifically designed for high-spin study, the large data set and the suppression of

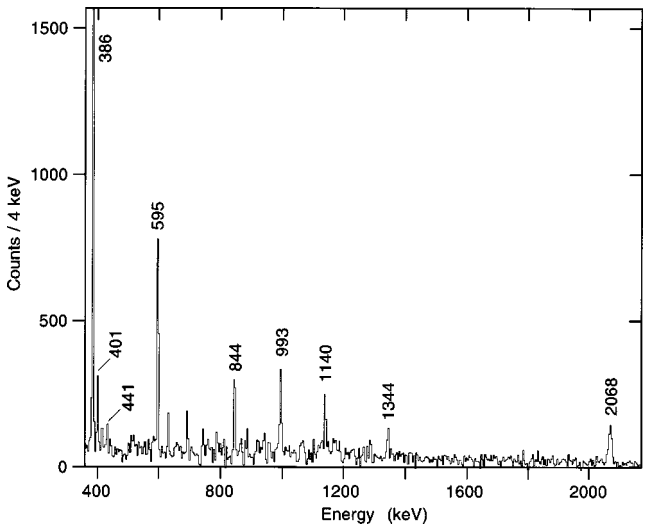

FIG. 5. A coincidence window set on the 266-keV gamma ray of the proposed new negative parity band.

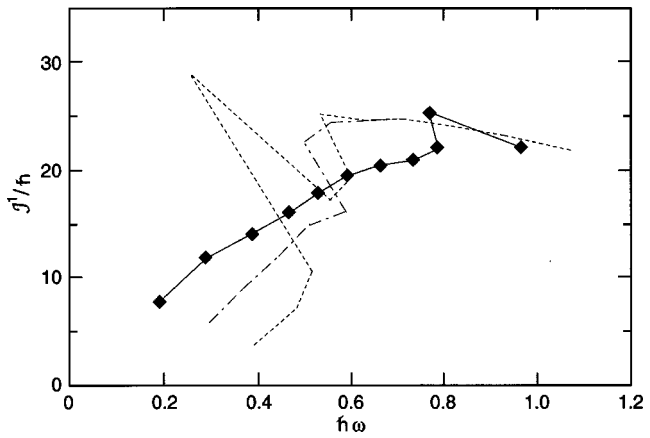

FIG. 6. The kinematic moment of inertia of the yrast sequence in ^{80}Sr (solid line) compared to neighboring ^{82,84}Sr (Refs. [24,28]) (^{82}Sr is the dash-dot line; ^{84}Sr is the short-dashed line). All show abrupt discontinuities arising from shape changes and alignment of $g_{9/2}$ particles, but for ^{80}Sr this effect is delayed to higher spin, due to the substantial gap in the single-particle energies at neutron number $N=38$.

competing reaction channels allowed the decay scheme of ^{80}Sr to be developed to surprisingly high spin. Figure 3 shows the yrast sequence above spin $J=8$ and the states decaying into the ground-state band. The mean feeding into discrete lines was $J=10$. A sample of the γ-γ coincidence data is shown in Fig. 1, a gate on the 1578-keV $J=18\rightarrow16$ ground-state band transition. Below this point, the ground-state cascade is clear, while above the cascade forks at least four different ways, two branches carrying approximately equal intensity. Both of these paths show backbends, a major change from the smooth development at lower spin. This observation is unambiguous in our work. The yrast line in this work above $J=18$ differs considerably from that of Davie *et al.* [4] and removes the puzzle of the jagged high-spin dynamic moment of inertia which was reported in that study and widely discussed as a possible signature of pairing collapse. Overall, the high-spin decay pattern found in the present study is similar to that suggested by Winchell *et al.* [7], including the forking above spin $J=18$. We could not confirm the Winchell structures labeled ''*b*,'' ''*c*,'' and ''*d*'' in our data, but did verify their structure of SB4. It is difficult to understand our nonobservation of Winchell's structure ''*c*'' as it was reported to feed into the yrast line at spin $J=14$, and we suggest it may be a misassignment associated with another nucleus. We did, however, observe the gamma rays in Winchell's ''*d*'' structure, and can confirm they are in ^{80}Sr, but were unable to place them in the decay scheme.

We also found many other high-energy decays to the yrast line which have not previously been reported. Most of the high-energy decays we find seem consistent with quadrupole radiation, except where otherwise noted in Table I or Figs. 2 and 3. At high spin, the gap between the yrast and yrare states of the same spin and parity is dramatically reduced. Presumably, this is a manifestation of the overall reduction of the importance of pairing due to blocking above the energy required for quasiparticle excitation. Although the bandheads for two-quasiparticle excitation lie around 3 MeV, the bands all have moments of inertia larger than the ground-state band, and so become energetically more favored with spin until they intercept the ground-state band near spin $J=20$. It is interesting to note that the ''superdeformed'' bands, polarized to very large deformation by promotion of particles into the $h_{11/2}$ shell, continue this trend, with even larger moments of inertia and even larger relative gains in energy with spin. Although the excitation energy of these bands is not yet known, the lowest members of these bands cannot lie very far above their ''normal'' non-yrast counterparts found in this study, or else ''normal'' states would make the yrast line to extremely high spin, and superdeformed states would never become yrast. It is worth noting that one of the bands reported by Devlin [18], band SD4, seems to have a very anomalous moment of inertia, much smaller than the other superdeformed sequences, and indeed lower than many of the ''normal'' bands including the ground-state sequence.

The monotonic increase of the moment of inertia at lower spin, shown in Fig. 6, has been discussed in terms of alignments of $g_{9/2}$ protons and neutrons, in a near-prolate-shaped potential. However, the new high-spin abrupt change in moment of inertia appears to arise from a structure with completely different character becoming yrast. This is exactly what was predicted by Nazarewicz *et al.* many years ago [13], with a noncollective near oblate core with fully aligned particles producing a band which became energetically favored at spin $J=18$ until termination at spin $J=24$. It is also interesting that this jump to near-rigid moment of inertia occurs at relatively high spin in ^{80}Sr, compared to other neighboring nuclei, again due to the importance of the $N,Z=38,40$ shell gaps keeping near-prolate shapes favored to high spin.

IV. CONCLUSION

This paper reports a detailed investigation of ^{80}Sr. The key to the experiment was having a data set which consisted almost exclusively ($>$97%) of gamma rays from a single

nucleus, diminishing the possibility of doublets with transitions from other nuclei which might cause confusing coincidence relationships and misleading angular distributions. Many new transitions and structures have been found, and previous spin and parity discrepancies resolved. The gamma band has now been firmly established, with both odd- and even-spin members identified. Its bandhead at 1141 keV distinguishes it from the many quasiparticle excited bands which have been found to start near 3 MeV. However, as soon as there is enough energy to allow quasiparticle excitation, very many configurations become possible, and now more than ten such states have been observed. Many of them seem to have larger moments of inertia than the ground state, due to both polarization and pairing suppression, so they approach the yrast line with increasing spin. By spin $J=18$ all the rotational simplicity is lost and the collectivity becomes fragmented amongst many levels. Consequently, it becomes difficult to follow the ''normal'' states to the shell-model termination in this space near spin $J=30$. One particular configuration, predicted to be of oblate shape with aligned $g_{9/2}$ protons and neutrons, appears to cause a sharp backbend above spin $J=18$ in the yrast line.

ACKNOWLEDGMENTS

This work was supported by the U.S. Department of Energy under Contract No. W-31-109-ENG-38. T. A. Sienko acknowledges a grant from the Undergraduate Research Program at Purdue University Calumet.

[1] E. Nolte, Y. Shida, W. Kutschera, R. Prestele, and H. Morinaga, Z. Phys. **268**, 267 (1974).
[2] C. J. Lister, B. J. Varley, H. G. Price, and J. W. Olness, Phys. Rev. Lett. **49**, 308 (1982).
[3] L. V. Theisen, S. L. Tabor, L. R. Medsker, G. Neuschaefer, L. H. Fry, Jr., and J. S. Clements, Phys. Rev. C **25**, 1325 (1982).
[4] R. F. Davie, D. Sinclair, S. S. L. Ooi, N. Poffé, and A. E. Smith, Nucl. Phys. **A463**, 683 (1987).
[5] K. E. G. Löbner, U. Lenz, U. Quade, K. Rudolph, W. Schomburg, S. J. Skorka, and M. Steinmayer, Nucl. Instrum. Methods Phys. Res. B **26**, 301 (1987).
[6] J. Heese, K. P. Lieb, S. Ulbig, B. Wörmann, J. Billowes, A. A. Chishti, W. Gelletly, C. J. Lister, and B. J. Varley, Phys. Rev. C **41**, 603 (1990).
[7] D. Winchell, V. Q. Wood, J. X. Saladin, I. Birriel, C. Baktash, M. J. Brinkman, H.-Q. Jin, D. Rudolph, C.-H. Yu, M. Devlin, D. R. LaFosse, F. Lerma, D. G. Sarantites, G. Sylvan, S. L. Tabor, R. M. Clark, P. Fallon, I. Y. Lee, and A. O. Macchiavelli, Phys. Rev. C **61**, 044322 (2000).
[8] C. J. Lister, P. E. Haustein, D. E. Alburger, and J. W. Olness, Phys. Rev. C **24**, 260 (1981).
[9] S. Della Negra, H. Gauvin, D. Jacquet, and Y. Le Beyec, Z. Phys. A **307**, 305 (1982).
[10] J. Döring, A. Aprahamian, R. C. de Haan, J. Görres, H. Schatz, M. Wiescher, W. B. Walters, L. T. Brown, C. N. Davids, C. J. Lister, and D. Seweryniak, Phys. Rev. C **59**, 59 (1999).
[11] P. Moller and J. R. Nix, At. Data Nucl. Data Tables **26**, 165 (1981).
[12] S. Aberg, Phys. Scr. **25**, 23 (1982).
[13] W. Nazarewicz, J. Dudek, R. Bengtsson, T. Bengtsson, and I. Ragnarsson, Nucl. Phys. **A435**, 397 (1985).
[14] P. Bonche, H. Flocard, P. H. Heenen, S. J. Kreiger, and M. S. Weiss, Nucl. Phys. **A443**, 39 (1985); **A523**, 300 (1991); **A530**, 149 (1991).
[15] K. Heyde, J. Moreau, and M. Waroqier, Phys. Rev. C **29**, 1859 (1984).
[16] W. Koepf and P. Ring, Nucl. Phys. **A511**, 279 (1990).
[17] D. Bucurescu, G. Căta, D. Cutoiu, G. Constantinescu, M. Ivascu, and N. Z. Zamfir, Nucl. Phys. **A401**, 22 (1983).
[18] M. Devlin *et al.*, Phys. Lett. B **415**, 328 (1997); Phys. Rev. Lett. **83**, 5447 (1999).
[19] L. M. Bollinger, R. C. Pardo, K. W. Shepard, P. J. Billquist, J. M. Bogaty, B. E. Clifft, R. Harkewicz, F. H. Munson, J. A. Nolen, and G. P. Zinkann, Nucl. Instrum. Methods Phys. Res. B **79**, 753 (1993).
[20] I. Y. Lee, Nucl. Phys. **A520**, 641c (1990).
[21] C. N. Davids, B. B. Back, K. Bindra, D. J. Henderson, W. Kutschera, T. Lauritsen, Y. Nagame, P. Sugathan, A. V. Ramayya, and W. B. Walters, Nucl. Instrum. Methods Phys. Res. B **70**, 358 (1992).
[22] J. P. Greene, C. J. Lister, P. Reiter, G. E. Thomas, and K. L. Unterzuber, Nucl. Instrum. Methods Phys. Res. A **495**, 334 (2001).
[23] J. Döring, R. A. Kaye, A. Aprahamian, M. W. Cooper, J. Daly, C. N. Davids, R. C. de Haan, J. Görres, S. R. Lesher, J. J. Ressler, D. Seweryniak, E. J. Stech, A. Susalla, S. L. Tabor, J. Uusitalo, W. B. Walters, and M. Wiescher, Phys. Rev. C **67**, 014315 (2003).
[24] S. L. Tabor, J. Döring, J. W. Holcomb, G. D. Johns, T. D. Johnson, T. J. Petters, M. A. Riley, and P. C. Womble, Phys. Rev. C **49**, 730 (1994).
[25] H. Sun, J. Döring, G. D. Johns, R. A. Kaye, G. Z. Solomon, S. L. Tabor, M. Devlin, D. R. LaFosse, F. Lerma, D. G. Sarantites, C. Baktash, D. Rudolph, C.-H. Yu, I. Y. Lee, A. O. Macchiavelli, I. Birriel, J. X. Saladin, D. F. Winchell, V. Q. Wood, and I. Ragnarsson, Phys. Rev. C **59**, 655 (1999).
[26] J. Döring, V. A. Wood, J. W. Holcomb, G. D. Johns, T. D. Johnson, M. A. Riley, G. N. Sylvan, P. C. Womble, and S. L. Tabor, Phys. Rev. C **52**, 76 (1995).
[27] N. V. Zamfir and R. F. Casten, Phys. Lett. B **260**, 265 (1991).
[28] D. Rudolph, C. Baktash, C. J. Gross, W. Satula, R. Wyss, I. Birriel, M. Devlin, H.-Q. Jin, D. R. LaFosse, F. Lerma, J. X. Saladin, D. G. Sarantites, G. N. Sylvan, S. L. Tabor, D. F. Winchell, V. Q. Wood, and C. H. Yu, Phys. Rev. C **56**, 98 (1997).
[29] S. Gerbick, R. A. Kaye, J. Döring, T. Baldwin, D. Campbell, K. Chandler, M. W. Cooper, C. Hoffman, J. Pavan, M. Wiedeking, and S. L. Tabor, Bull. Am. Phys. Soc. **46**, 100 (2001).